Strictly linear polyethylene using Co-catalysts chelated by fused bis(arylimino)pyridines: probing *ortho*-cycloalkyl ring-size effects on molecular weight

Hongyi Suo,[a,b] Ivan I. Oleynik,[c*] Chantsalnyam Bariashir,[a,b] Irina V. Oleynik,[c] Zheng Wang,[a,b] Gregory A. Solan,*[a,d] Yanping Ma,[a] Tongling Liang[a] and Wen-Hua Sun[a,b]*

[a] Key Laboratory of Engineering Plastics and Beijing National Laboratory for Molecular Sciences, Institute of Chemistry, Chinese Academy of Sciences, Beijing 100190, China.

[b] CAS Research/Education Center for Excellence in Molecular Sciences, University of Chinese Academy of Sciences, Beijing 100049, China.

[c] N.N. Vorozhtsov Novosibirsk Institute of Organic Chemistry, Pr. Lavrentjeva 9, Novosibirsk 630090, Russia.

[d] Department of Chemistry, University of Leicester, University Road, Leicester LE1 7RH, UK.

* Correspondence: oleynik@nioch.nsc.ru, gas8@leicester.ac.uk and whsun@iccas.ac.cn

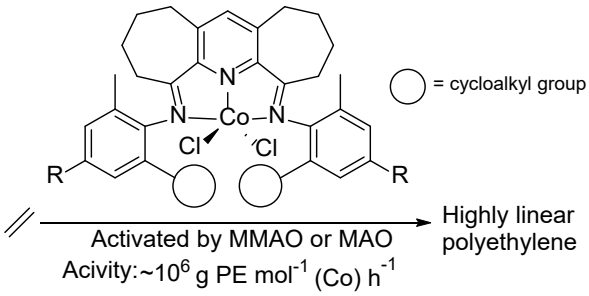

Abstract

Six examples of α,α'-bis(arylimino)-2,3:5,6-bis(pentamethylene)pyridine-cobalt(II) chlorides, [2,3:5,6-{$C_4H_8C(NAr)$}$_2C_5HN$]$CoCl_2$ (Ar = 2-(C_5H_9)-6-MeC_6H_3 **Co1**, 2-(C_6H_{11})-6-MeC_6H_3 **Co2**, 2-(C_8H_{15})-6-MeC_6H_3 **Co3**, 2-(C_5H_9)-4,6-$Me_2C_6H_2$ **Co4**, 2-(C_6H_{11})-4,6-$Me_2C_6H_2$ **Co5**, 2-(C_8H_{15})-4,6-$Me_2C_6H_2$ **Co6**), containing N-aryl groups that differ in either the ring size of the *ortho*-cycloalkyl substituents or the *para*-R group (R = H, Me), have been synthesized using a one-pot template approach. The molecular structure of **Co1** highlights the ring puckering of both the *ortho*-cyclopentyl substituents and the two pyridine-fused seven-membered rings; a square-based pyramidal geometry is conferred about the metal center. On activation with either methylaluminoxane (MAO) or modified MAO (MMAO), all six complexes afforded strictly linear polyethylene (all T_m's > 130 ºC) with high molecular weight (M_w up to 64.3 kg mol^{-1}). Furthermore, all precatalysts displayed high activities (up to 2 × 10^6 g PE mol^{-1} (Co) h^{-1}) at temperatures between 20 – 60 ºC with the catalytic activities correlating with the type of *ortho*-cycloalkyl substituent: cyclohexyl (**Co2**, **Co5**) > cyclopentyl (**Co1**, **Co4**) > cyclooctyl (**Co6**, **Co3**) for either R = H or Me. The narrow unimodal distributions of the resulting polymers are consistent with single-site active species for the catalysts.

Keywords: linear polyethylene; *ortho*-cycloalkyl substituent; coordination polymerization

1. Introduction

The use of late transition metal complexes as homogeneous catalysts in alkene oligo-/polymerization catalysis has been extensively explored since the mid to late 1990s and remains an active field of research to this day [1-4]. In particular, the ability of bis(imino)pyridine-iron and -cobalt complexes (**A**, in Chart 1) to mediate the formation of either high density polyethylene or α-olefins has provided the impetus for both academic and industrial research [5-8]. While multiple factors influence the performance of the catalyst, the structural features of the bis(arylimino)pyridine ligand are integral allowing control of the catalytic activity and the molecular weight of the oligo-/polymer [9-19]. Of particular note, the positioning of alkyl substituents (*e.g.*, methyl, isopropyl *etc*.) at the *ortho*-positions of the two N-aryl groups of the catalyst and the resulting protection of the active species offers a means of regulating the molecular weight of the polymer. Indeed, recognition of such structural features has inspired the development of numerous other compatible N,N,N-ligand sets [20-24]. Common to both iron and cobalt catalysts is a selectivity for highly linear polyethylene, with cobalt catalysts generally showing narrower molecular weight distributions while their iron counterparts display superior activities along with higher molecular weight polymers.

Lately, we have been interested in developing bis(imino)pyridine ligand sets that incorporate fused carbocyclic rings with the intent of introducing structural rigidity to the pincer ligand framework by reducing the flexibility of the exterior imine donors [8,25]. With regard to cobalt precatalysts, both singly and doubly fused derivatives with ring sizes of between six and eight are accessible (see for example **B** − **E**, Chart 1) [16,18,25-27]. In terms of catalytic performance, high activities and improved thermal stabilities are a general feature of these systems, while the number of fused rings as well as ring size can be influential on the molecular weights of the olefinic products. For example, using doubly fused **B** as the precatalyst (Chart 1) [25], an undesirable mixture of polymers and oligomers are obtained, while use of the singly fused **C** (Chart 1) [26] leads to solely polymers with narrower molecular weight distribution. Increasing the ring size to seven (**D** and **E**, Chart 1) [16, 18], results in increased molecular weight which is most apparent

with doubly-fused **E** [18].

<Chart 1>

Given the predilection of **E**-type cobalt precatalysts to form higher molecular weight polyethylene, we wanted to explore how the introduction of more sterically hindered *ortho* groups would impact on the molecular weight and other properties of the polymer. In particular, we describe the catalytic performance of a series of α,α'-bis(arylimino)-2,3:5,6-bis(pentamethylene)pyridine-cobalt(II) chloride complexes that contain cycloalkyl *ortho*-substituents of various ring sizes (cyclopentyl *vs*. cyclohexyl *vs*. cyclooctyl); electronic variations imparted by different *para*-R groups (H, Me: Chart 1) presents a further feature to be investigated. Elsewhere, *ortho*-cycloalkyl incorporation has been shown to have some notable effects on catalytic performance and molecular weight which have been correlated with the size of cyclic substituent [28-31]. Full characterization of the complexes and intrinsic properties of the resulting polyethylenes (*e.g.*, molecular weight, distribution, melting temperatures, crystallinity, microstructure and water contact angle) are reported.

2. Materials and Methods

2.1 General considerations

All manipulations of air- and/or moisture-sensitive compounds were carried out under a nitrogen atmosphere using standard Schlenk techniques. Toluene was refluxed over sodium benzophenone and distilled under nitrogen prior to use. Methylaluminoxane (MAO, 1.46 M solution in toluene) and modified methylaluminoxane (MMAO, 2.0 M in heptane) were purchased from Akzo Nobel Corp. High-purity ethylene was purchased from Beijing Yansan Petrochemical Co. and used as received. Other reagents were purchased from Aldrich, Acros or local suppliers. IR spectra were recorded on a Perkin-Elmer System 2000 FT-IR spectrometer. Elemental analysis was carried out using a Flash EA 1112 microanalyzer. Molecular weights and molecular weight distributions of the polyethylenes were determined using a PL-GPC220 instrument at 150 ºC with 1,2,4-trichlorobenzene as solvent. Melting temperatures of the polyethylenes were measured from the second scanning run on a Perkin-Elmer DSC-7

differential scanning calorimeter (DSC) under a nitrogen atmosphere. In the procedure, a sample of about 5.0 mg was heated to 160 ºC at a rate of 20 ºC/min and kept for 2 min at 160 ºC to remove the thermal history and then cooled to 20 ºC at a rate of 20 ºC /min. The ^{13}C NMR spectra of the polyethylenes were recorded on a Bruker DMX-300 MHz instrument at 135 ºC in deuterated 1,1,2,2-tetrachloroethane-d_2 with TMS as an internal standard. The water contact angles (WCAs) were determined using a contact angle tester (Harke-Spcax1). The compounds, α,α'-dioxo-2,3:5,6-bis(pentamethylene)pyridine [18], 2-cyclopentyl-6-methylaniline hydrochloride, 2-cyclohexyl-6-methylaniline hydrochloride, 2-cyclooctyl-6-methylaniline hydrochloride, 2-cyclopentyl-4,6-dimethylaniline hydrochloride, 2-cyclohexyl-4,6-dimethylaniline hydrochloride, 2-cyclooctyl-4,6-dimethylaniline hydrochloride, have been prepared using literature methods [32].

2.2 Preparation of 2,3:5,6-{$C_4H_8C(NAr)\}_2C_5HN$]$CoCl_2$

(a) Ar = 2-(C_5H_9)-6-MeC_6H_3 (**Co1**). A suspension of α,α'-dioxo-2,3:5,6-bis(pentamethylene) pyridine (0.122 g, 0.5 mmol), 2-cyclopentyl-6-methylaniline hydrochloride (0.212 g, 1.0 mmol) and $CoCl_2$ (0.058 g, 0.45 mmol) in glacial acetic acid (10 mL) was stirred and heated to reflux for 6 h. On cooling to room temperature, an excess of diethyl ether was added to precipitate the product. The precipitate was then filtered and washed with diethyl ether (3 × 15 mL) and dried under reduced pressure to give **Co1** as a green powder (0.18 g, 59%). FT-IR (cm^{-1}): 2921 (s), 2857 (m), 1610 (m), 1582 (m), 1440 (s), 1330 (w), 1250 (m), 1210 (m), 1169 (m), 1132 (m), 1036 (m), 931 (w), 854 (s), 754 (w). $C_{39}H_{47}Cl_2CoN_3$ (687.66): calcd. C 68.12, H 6.89, N 6.11%; found C 68.39, H 6.99, N 6.02%.

(b) Ar = 2-(C_6H_{11})-4-MeC_6H_3 (**Co2**). Based on the molar ratios and procedure described for the synthesis of **Co1**, **Co2** was obtained as a green powder (0.14 g, 42%). FT-IR (cm^{-1}): 2925 (s), 2851 (m), 1608 (m), 1582 (m), 1447 (s), 1320 (w), 1250 (m), 1169 (m), 1134 (m), 1036 (m), 931 (w), 779 (s). $C_{41}H_{51}Cl_2CoN_3$ (715.71): calcd. C 68.81, H 7.18, N 5.87%; found C 68.50, H 7.09, N 5.78%.

(c) Ar = 2-(C_8H_{15})-6-MeC_6H_3 (**Co3**). Based on the molar ratios and procedure described for the synthesis of **Co1**, **Co3** was obtained as a green powder (0.22 g, 64%). FT-IR (cm^{-1}): 2937 (s),

2851 (m), 1699 (w), 1609 (m), 1585 (m), 1450 (s), 1340 (w), 1252 (m), 1191 (m), 1169 (m), 1135 (m), 1035 (m), 929 (w), 776 (s). $C_{45}H_{59}Cl_2CoN_3$ (771.82): calcd. C 70.03, H 7.71, N 5.44%; found C 70.15, H 7.34, N 5.38%.

(d) Ar = 2-(C_5H_9)-4,6-$Me_2C_6H_2$ (**Co4**). Based on the molar ratios and procedure described for the synthesis of **Co1**, **Co4** was obtained as a green powder (0.17 g, 53%). FT-IR (cm^{-1}): 2920 (s), 2864 (s), 1609 (m), 1589 (m), 1474 (s), 1448 (s), 1384 (w), 1252 (w), 1167 (w), 1132 (w), 1034 (w), 961 (w), 854 (m), 755 (w). $C_{41}H_{51}Cl_2CoN_3$ (715.71): calcd. C 68.81, H 7.18, N 5.87%; found C 68.68, H 7.01, N 5.75%.

(e) Ar = 2-(C_6H_{11})-4,6-$Me_2C_6H_2$ (**Co5**). Based on the molar ratios and procedure described for the synthesis of **Co1**, **Co5** was obtained as a green powder (0.21 g, 62%). FT-IR (cm^{-1}): 3051 (w), 2851 (m), 1649 (w), 1610 (m), 1560 (m), 1481 (m), 1447 (s), 1339 (w), 1253 (m), 1169 (m), 1129 (m), 1021 (m), 923 (w), 850 (s), 757 (m). $C_{43}H_{55}Cl_2CoN_3$ (743.77): calcd. C 69.44, H 7.45, N 5.65%; found C 69.12, H 7.39, N 5.54%.

(f) Ar = 2-(C_8H_{15})-4,6-$Me_2C_6H_2$ (**Co6**). Based on the molar ratios and procedure described for the synthesis of **Co1**, **Co6** was obtained as a green powder (0.20 g, 55%). FT-IR (cm^{-1}): 2925 (s), 2856 (m), 1603 (m), 1550 (m), 1450 (s), 1340 (m), 1252 (m), 1211 (m), 1168 (m), 1132 (m), 1036 (w), 928 (w), 855 (s), 753 (m). $C_{47}H_{63}Cl_2CoN_3$ (799.88): calcd. C 70.58, H 7.94, N 5.25%; found C 70.77, H 8.05, N 5.11%.

2.3 X-ray crystallographic studies

Single crystals of **Co1** suitable for the X-ray diffraction analysis were obtained by layering a dichloromethane solution of the corresponding complex with hexane at room temperature in air. With graphite monochromated Mo-Kα radiation (λ = 0.71073 Å) at 173(2) K, cell parameters were obtained by global refinement of the positions of all collected reflections. Intensities were corrected for Lorentz and polarization effects and empirical absorption. The structures were solved by direct methods and refined by full-matrix least squares on F^2. All hydrogen atoms were placed in calculated positions. Structure solution and structure refinement were performed by using the SHELXT (Sheldrick, 2015) [33,34]. The disorder displayed by the cycloheptyl and solvent molecule was also processed by the SHELXL (Sheldrick, 2015) [34]. Details of the X-

ray structure determinations and refinements are provided in Table S1 (see SI).

2.3 Polymerization studies

Ethylene polymerization at 1 atm ethylene pressure. The polymerization at 1 atm ethylene pressure was carried out in a 100 mL Schlenk tube. Under an ethylene atmosphere, **Co3** (3 μmol) was added followed by toluene (30 mL) and then the required amount of co-catalyst (MAO, MMAO) introduced by syringe. The solution was then stirred at 30 ºC under 1 atm of ethylene pressure. After 30 min, the ethylene pressure was vented and solution quenched with 10% hydrochloric acid in ethanol. The polymer was washed with ethanol, dried under reduced pressure at 60 ºC and then weighed.

Ethylene polymerization at 10 atm ethylene pressure. The polymerization at 10 atm ethylene pressure was carried out in a stainless steel autoclave (0.25 L) equipped with an ethylene pressure control system, a mechanical stirrer and a temperature controller. The autoclave was evacuated and backfilled with ethylene three times. When the required temperature was reached, the precatalyst (3.0 μmol) was dissolved in toluene (25 mL) in a Schlenk tube and injected into the autoclave containing ethylene (~ 1 atm) followed by the addition of more toluene (25 mL). The required amount of co-catalyst (MAO and MMAO) and additional toluene were added successively by syringe taking the total volume of toluene to 100 mL. The autoclave was immediately pressurized with 10 atm pressure of ethylene and the stirring commenced. After the required reaction time, the reactor was cooled with a water bath and the ethylene pressure vented. Following quenching of the reaction with 10% hydrochloric acid in ethanol, the polymer was collected and washed with ethanol and dried under reduced pressure at 60 ºC and weighed.

3. Results and Discussion

3.1 Synthesis and characterization

Reaction of α,α'-dioxo-2,3:5,6-bis(pentamethylene) with the corresponding aniline hydrochloride and cobalt chloride in acetic acid at reflux gave [2,3:5,6-{$C_4H_8C(NAr)$}$_2C_5HN$]$CoCl_2$ (Ar = 2-(C_5H_9)-6-MeC_6H_3 **Co1**, 2-(C_6H_{11})-6-MeC_6H_3 **Co2**, 2-(C_8H_{15})-6-MeC_6H_3 **Co3**, 2-(C_5H_9)-4,6-$Me_2C_6H_2$ **Co4**, 2-(C_6H_{11})-4,6-$Me_2C_6H_2$ **Co5**, 2-(C_8H_{15})-

4,6-$Me_2C_6H_2$ **Co6**] in good yield (Scheme 1). Such a one-pot methodology was deemed necessary as attempts to form the free bis(imino)pyridine proved unsuccessful [16,18,27,35]. Complexes **Co1** – **Co6** were characterized by FTIR spectroscopy, elemental analysis and, in the case of **Co1**, by single crystal X-ray diffraction.

<Scheme 1>

Crystals of **Co1** suitable for the X-ray determination were grown by slow diffusion of hexane into a dichloromethane solution of the corresponding complex. A view of the structure is shown in Figure 1; selected bond lengths and angles are listed in the caption. The structure consists of a single cobalt center surrounded by three nitrogen atoms belonging to the tridentate ligand and two chlorides (Cl2) to form a geometry that can be best described as square-based pyramidal. Specifically, Cl1 occupies the apical position while the basal plane is filled by N(1), N(2), N(3) and Cl2 with the Co atom sitting 0.514 Å above this plane; structurally related analogues have been reported [5, 16-18, 27]. The two five-membered chelate rings incorporating the tridentate ligand show some deviation from planarity which is best highlighted by the N3-C2-C1-Co1 and N1-C15-C14-N2 torsion angles of 7.37° and -6.76°, respectively. As is common to many bis(imino)pyridine-cobalt(II) complexes, the central Co-$N_{pyridine}$ bond length [2.087(4) Å] is shorter than the exterior Co-N_{imine} bond lengths [2.169(5) Å and 2.174(4) Å] [18, 25]. Within the saturated sections of the fused seven-membered rings (C3-C4-C5-C6 and C10-C11-C12-C13), single bond character is apparent with bond distances ranging from 1.496(8) to 1.545(12) Å, while the corresponding bond angles exhibit sp^3-hybridization [25]. The sterically bulky *ortho*-cyclopentyl substituents adopt envelope conformations which results in some tilting of the N-aryl groups with respect to the neighboring imine vectors (dihedral angles = 69.55° and 83.57°). The C2-N3 and C14-N2 bond lengths [1.282(7) Å and 1.291(8) Å] are consistent with C=N double-bond character. There are no intermolecular contacts of note.

<Figure 1>

In the IR spectra of **Co1** – **Co6** strong peaks around 1600 cm^{-1} are evident which can

be attributed to the C=N stretching vibrations belonging to the coordinated imines [16, 18, 27]. Furthermore, the microanalytical data for the complexes were in full agreement with elemental compositions of general formula $LCoCl_2$.

3.2 Catalyst evaluation for ethylene polymerization

Complexes **Co1** – **Co6**, have all been systematically investigated as precatalysts for ethylene polymerization using either methylaluminoxane (MAO) or modified methylaluminoxane (MMAO) as co-catalyst [16, 18, 25-27, 36]. For each aluminoxane, **Co3** was selected as the test precatalyst and variations of Al/Co molar ratio, reaction temperature and run time were all investigated as part of the catalyst optimization; the results are compiled in Tables 1 and 2. In general, the polyethylenes were characterized by gel permeation chromatography (GPC) and different scanning calorimetry (DSC) as well as by high temperature NMR spectroscopy.

Optimization of reaction conditions using Co3/MMAO

Firstly, the effects of temperature on the performance of **Co3**/MMAO were investigated over the range 20 to 60 ºC with the Al/Co molar ratio maintained at 2000 and the pressure of ethylene at ten atmospheres (Table 1). The highest activity of 1.91×10^6 g PE mol^{-1} (Co) h^{-1} was obtained at 20 ºC (entry 1, Table 1), above which it sharply decreased reaching a minimum of 0.27×10^6 g PE mol^{-1} (Co) h^{-1} at 60 ºC (entry 5, Table 1). The molecular weights of the corresponding polymers followed a similar downward trend with increasing temperature (Fig. 2a), a finding that can be attributed to faster chain termination at higher temperature.

Secondly, with the temperature fixed at 20 ºC, the Al/Co molar ratio was systematically varied between 1000 and 3000 with the maximum activity reached with 2000 molar equivalents (entry 1, Table 1). Between 1000 and 2250, the M_w's of the polyethylenes gradually decreased from 61.3 to 42.6 kg mol^{-1} (Fig. 2b), a result that can be likely ascribed to increased chain transfer occurring from cobalt to aluminum as a consequence of the larger amounts of alkyl aluminum reagent employed [5, 8, 37]. Interestingly, with the molar ratios between 2500 and 3000, a dramatic increase in molecular weight was observed with values reaching as high as 53.8 kg mol^{-1} with 3000 equivalents of MMAO. It would seem plausible that the formation of a new active

species has occurred within this molar ratio window, a similar observation has been noted elsewhere [26].

Thirdly, to determine the catalyst lifetime, the polymerization runs were performed over different intervals with the highest activity of 2.00 × 10^6 g PE mol^{-1} (Co) h^{-1} observed after 15 minutes (entry 12, Table 1). When the run time was extended to 60 minutes (entry 14, Table 1), only *ca.* 50% loss of activity was observed, highlighting the stability and slow deactivation of this catalyst. In terms of molecular weight, longer reactions were accompanied by an increase in M_w from 43.5 to 52.4 kg mol^{-1} (Fig. 2c).

The effect of ethylene pressure was also found to be significant with the activity at one atmosphere being around one tenth of that observed at 10 atmospheres (entries 1 and 15, Table 1). On the other hand, the molecular weight remained essentially invariant. These results are consistent with both chain propagation and chain termination increasing equally with ethylene pressure [36, 38].

< Table 1>

<Figure 2>

Optimization of reaction conditions using Co3/MAO

To complement the study performed with MMAO, we also examined the performance of **Co3** using MAO as the co-catalyst. As before, the first stage of catalytic optimization focused on the effect of temperature (entries 1 – 5, Table 2). The maximum activity was achieved at 30 ºC (1.21 × 10^6 g PE mol^{-1} (Co) h^{-1}), above which the activity steadily lowered until at 60 ºC the activity had dropped almost threefold. At the same time, the molecular weight decreased significantly with increasing temperature from 53.1 to 18.2 kg mol^{-1} (see Fig. 3a).

With the temperature maintained at 30 ºC, the effect of varying the Al/Co molar ratio from 1000 to 3000 was studied. A peak in activity of 1.35 × 10^6 g PE mol^{-1} (Co) h^{-1} was identified with an Al/Co ratio of 1500 (entries 6 – 11, Table 2). Unlike with MMAO, no anomalous behavior was observed with the molecular weight steadily dropping as the ratio was increased from 1000 to 3000 in agreement with increased chain transfer from the active cobalt species to aluminum (see Fig. 3b) [8, 18, 27, 39-40]. With respect to run time, the performance of **Co3**/MAO mirrored

Co3/MMAO, with the activity gradually decreasing over time while the molecular weight increased (see Fig. 3c).

As noted earlier, the catalyst activity of **Co3**/MMAO was also found to drop markedly on reducing the ethylene pressure for 10 to 1 atmosphere, while the molecular weight of the material remained similar at either pressure. As a general feature common to both co-catalysts, the range in molecular weight and molecular weight distributions are comparable, while the activity using MAO is slightly lower, a finding that contrasts with that reported with structurally related cobalt analogs [18].

< Table 2>

<Figure 3>

Structural effects of precatalyst on polymerization using MMAO or MAO

To investigate the influence of structural variations of the precatalyst on catalyst performance and polymer properties, all six cobalt complexes, **Co1 – Co6**, were systematically studied. For the sake of comparison, the previously reported [2,3:5,6-{C_4H_8C(N(2,6-$Me_2C_6H_3$))}$_2C_5HN$]$CoCl_2$ (**Co$_{Me2Ph}$**, Scheme 1) was also included in the evaluation [18]. Firstly, using the optimized conditions established for **Co3**/MMAO [Al/Co = 2000, temperature = 20 ºC, run time = 30 minutes], **Co1** – **Co6**, on activation with MMAO, exhibited good activities in the range 1.31 – 2.22 × 10^6 g PE mol^{-1} (Co) h^{-1} that fall in the order: **Co5** (2-cyclohexyl-4,6-methyl) ~ **Co2** (2-cyclohexyl-6-methyl) > **Co1** (2-cyclopentyl-6-methyl) > **Co3** (2-cyclooctyl-6-methyl) > **Co4** (2-cyclopentyl-4,6-methyl) > **Co6** (2-cyclooctyl-4,6-methyl). With respect to the particular *para*-R group, **Co2** (2-cyclohexyl-6-methyl) > **Co1** (2-cyclopentyl-6-methyl) > **Co3** (2-cyclooctyl-6-methyl) for R^2 = H and **Co5** (2-cyclohexyl-4,6-methyl) > **Co4** (2-cyclopentyl-4,6-methyl) > **Co6** (2-cyclooctyl-4,6-methyl) for R^2 = Me. Several points emerge from examination of these findings. Firstly, the type of cycloalkyl group positioned at the *ortho*-position of the N-aryl group affects catalytic activity with the cyclohexyl systems giving the highest activities (**Co5**, **Co2**), while for a specific *para*-R group cyclooctyl shows the lowest (**Co3**, **Co6**). Secondly, the nature of the 4-R group is also influential on catalytic activity with the 4-H derivative more active than its 4-Me analog for the pairs **Co6**/**Co3** and **Co4**/**Co1**, though similar for **Co5**/**Co2**. To

explain the superior performance of the cyclohexyl systems it would seem plausible that the flexibility of the cyclohexyl ring provides the most suitable protection to the metal center in the active catalyst but does not impede the approach of the ethylene monomer. With respect to the molecular weight, values in the range 33.7 – 55.6 kg mol^{-1} were observed with the most bulky cyclooctyl-containing **Co3** and **Co6** affording polymer at the top end and cyclohexyl **Co5** and **Co2** the bottom, trends that are clearly the inverse of that found for activity. In comparison with **Co$_{Me2Ph}$**/MMAO, the *ortho*-cycloalkyl systems in general exhibited an order of magnitude higher molecular weight, although the catalytic activity is slightly lower (Fig. 4 left) [18].

With MAO as co-catalyst similar trends in activity and molecular weight are observed with the cyclohexyl systems (**Co5**, **Co2**) again showing the highest activity and the lowest molecular weight. By contrast, the cyclooctyl systems (**Co6**, **Co3**) give the lowest activity but the highest molecular weight (Table 3). By comparison, the catalytic activity of **Co$_{Me2Ph}$**/MAO is nearly twice as much as that seen for **Co2**, **Co4** and **Co5**, and almost five times that for **Co6**. As with MMAO-promoted polymerizations, the molecular weights obtained using **Co1** – **Co6** (range: 29.6 – 52.0 kg mol^{-1}) are all significantly higher than that seen for **Co$_{Me2Ph}$** (12.1 kg mol^{-1}) (Fig. 4, right).

As a common feature, regardless of MMAO or MAO activation, narrow unimodal distributions of the polymers are observed (PDI range: 1.86 – 4.23) consistent with single-site-like active species. In addition, high melting temperatures of the polymers (T_m values: 130 – 136 ºC) are supportive of the polyethylenes displaying high linearity [5], while their heat of fusion data indicate exceptionally high crystallinity (average 200 J/g *vs* 170 J/g for commercial HDPE). Comparatively, polymers obtained using **Co$_{Me2Ph}$**/MMAO or **Co$_{Me2Ph}$**/MAO gave lower T_m values (128.0 – 130.1 ºC) and heats of fusion data that fell at the lower end of the range.

<Table 3>

<Figure 4>

To provide further support for the linearity of the polymers, representative samples synthesized using **Co3**/MAO at 30 ºC (entry 10, Table 3), **Co3**/MMAO (entry 3, Table 3) at 20 ºC and **Co2**/MMAO at 20 ºC (entry 2, Table 3), were characterized by ^{13}C NMR spectroscopy (recorded in 1,1,2,2-tetrachloroethane-d_2 at 135 ºC). In each case high intensity singlets observed

around δ 30.00 (see Figs. 5, 6a and 6b) were the only signals detectable which can be assigned to the -$(CH_2)_n$- repeat unit in accord with high linearity [18, 27]. On the other hand, a sample of the polyethylene prepared using **Co6**/MMAO at 20 ºC (entry 6, Table 3) revealed on close inspection of the aliphatic region additional weak peaks at δ 32.23, 22.94 and 14.27 (peaks 3, 2, and 1 in Fig. 6) that could be attributed to *n*-propyl end-groups. Indeed, a lower molecular weight sample of polyethylene prepared using **Co3**/MMAO at 60 ºC (entry 5, in Table 1) again showed these low intensity *n*-propyl peaks (peaks 3, 2, and 1 in Fig. 7) [41]. However, examination of the downfield region in this spectrum revealed no evidence for peaks that could be assigned to unsaturated chain ends, which would suggest the absence of termination via *β*-H elimination and hence transfer to aluminum as the key termination pathway.

<Figure 5>

<Figure 6>

<Figure 7>

To further explore the properties of the polyethylenes, we also conducted a series of measurements concerned with their surface properties [42, 43, 44]. In this regard the value of the water contact angle (WCA) can be informative when put alongside the value of 101.4º for commercial sample of low-density polyethylene (LDPE) of high molecular weight ($M_w \approx 914.7$ kg mol^{-1}) and low T_m (107 ºC) [45]. For the polymer obtained at 60 ºC using **Co3**/MMAO (entry 5, Table 1), its WCA was determined as 110.3º, while for the polymers generated at 20 ºC, using **Co1**/MMAO (entry 1, Table 3) and **Co2**/MMAO (entry 2, Table 3), the WCA's were 109.8º and 111.8º, respectively. Generally, all the polymers studied exhibited superior hydrophobic properties when compared against the commercial sample of polyethylene.

<Figure 8>

4. Conclusions

A family of six cobalt(II) chloride complexes, **Co1** − **Co6**, bound by ring-fused α,α′-bis(cycloarylimino)-2,3:5,6-bis-(pentamethylene)pyridines, was systematically synthesized using a one-pot approach and fully characterized. On activation with either MMAO or MAO, all these *ortho*-cycloalkyl-containing complexes afforded strictly linear polyethylene with high

molecular weight and indeed around 40 kg mol^{-1} higher than that observed with a previously studied structural analog **Co$_{Me2Ph}$**. In terms of catalytic activity, the cyclohexyl-substituted catalysts (**Co2**, **Co5**) were higher than the cyclopentyl-containing catalysts (**Co1**, **Co4**) which were in-turn higher than the cyclooctyl-substituted ones (**Co3**, **Co6**). In general, the MMAO-promoted polymerizations showed higher activities than with their MAO counterparts.

Declarations of interest: none

Acknowledgements
This work was supported by the National Natural Science Foundation of China (Nos. U1362204 and 21611130026). GAS thanks the Chinese Academy of Sciences for a President's International Fellowship for Visiting Scientists.

References
[1] V.C. Gibson, S.K. Spitzmesser, Advances in non-metallocene olefin polymerization catalysis, Chem. Rev. 103 (2003) 283-316.
[2] G.J.P. Britovsek, V.C. Gibson, D.F. Wass, The search for new-generation olefin polymerization catalysts: Life beyond metallocenes, Angew. Chem. Int. Ed. 38 (1999) 428-447.
[3] S.D. Ittel, L.K. Johnson, M. Brookhart, Late-metal catalysts for ethylene homo- and copolymerization, Chem. Rev. (Washington, DC, U. S.) 100 (2000) 1169-1203.
[4] Z. Wang, G.A. Solan, W. Zhang, W.-H. Sun, Carbocyclic-fused *N*,*N*,*N*-pincer ligands as ring-strain adjustable supports for iron and cobalt catalysts in ethylene oligo-/polymerization, Coord. Chem. Rev. 363 (2018) 92-108.
[5] B.L. Small, M. Brookhart, A.M.A. Bennett, Highly active iron and cobalt catalysts for the polymerization of ethylene, J. Am. Chem. Soc. 120 (1998) 4049-4050.
[6] G.J.P. Britovsek, V.C. Gibson, S.J. McTavish, G.A. Solan, A.J.P. White, D.J. Williams, G.J.P. Britovsek, B.S. Kimberley, P.J. Maddox, Novel olefin polymerization catalysts based on iron and cobalt, Chem. Commun. (1998) 849-850.
[7] B.L. Small, M. Brookhart, Iron-based catalysts with exceptionally high activities and selectivities for oligomerization of ethylene to linear α-olefins, J. Am. Chem. Soc. 120 (1998) 7143-7144.
[8] G.J.P. Britovsek, M. Bruce, V.C. Gibson, B.S. Kimberley, P.J. Maddox, S. Mastroianni, S.J. McTavish, C. Redshaw, G.A. Solan, S. Strömberg, A.J.P. White, D.J. Williams, Iron and cobalt ethylene polymerization catalysts bearing 2,6-bis(imino)pyridyl ligands: Synthesis, structures, and polymerization studies, J. Am. Chem. Soc. 121 (1999) 8728-8740.
[9] C. Bianchini, G. Giambastiani, I.G. Rios, G. Mantovani, A. Meli, A.M. Segarra, Ethylene oligomerization, homopolymerization and copolymerization by iron and cobalt catalysts with 2,6-(bis-organylimino)pyridyl ligands, Coord. Chem. Rev. 250 (2006) 1391-1418.
[10] G.J.P. Britovsek, S. Mastroianni, G.A. Solan, S.P.D. Baugh, C. Redshaw, V.C. Gibson, A.J.P. White, D.J. Williams, M.R.J. Elsegood, Oligomerisation of ethylene by

bis(imino)pyridyliron and -cobalt complexes, Chem. Eur. J. 6 (2000) 2221-2231.
[11] V.C. Gibson, C. Redshaw, G.A. Solan, Bis(imino)pyridines: Surprisingly reactive ligands and a gateway to new families of catalysts, Chem. Rev. 107 (2007) 1745-1776.
[12] G.J.P. Britovsek, V.C. Gibson, B.S. Kimberley, S. Mastroianni, C. Redshaw, G.A. Solan, A.J.P. White, D.J. Williams, Bis(imino)pyridyl iron and cobalt complexes: The effect of nitrogen substituents on ethylene oligomerisation and polymerisation, J. Chem. Soc., Dalton Trans. (2001) 1639-1644.
[13] G.J.P. Britovsek, V.C. Gibson, O.D. Hoarau, S.K. Spitzmesser, A.J.P. White, D.J. Williams, Iron and cobalt ethylene polymerization catalysts: Variations on the central donor, Inorg. Chem. 42 (2003) 3454-3465.
[14] L. Guo, H. Gao, L. Zhang, F. Zhu, Q. Wu, An unsymmetrical iron(II) bis(imino)pyridyl catalyst for ethylene polymerization: Effect of a bulky ortho substituent on the thermostability and molecular weight of polyethylene, Organometallics 29 (2010) 2118-2125.
[15] Z. Flisak, W.-H. Sun, Progression of diiminopyridines: From single application to catalytic versatility, ACS Catal. 5 (2015) 4713-4724.
[16] F. Huang, W. Zhang, E. Yue, T. Liang, X. Hu, W.H. Sun, Controlling the molecular weights of polyethylene waxes using the highly active precatalysts of 2-(1-aryliminoethyl)-9-arylimino-5,6,7,8-tetrahydrocycloheptapyridylcobalt chlorides: Synthesis, characterization, and catalytic behavior, Dalton Trans. 45 (2016) 657-666.
[17] F. Huang, W. Zhang, Y. Sun, X. Hu, G.A. Solan, W.-H. Sun, Thermally stable and highly active cobalt precatalysts for vinyl-polyethylenes with narrow polydispersities: Integrating fused-ring and imino-carbon protection into ligand design, New J. Chem. 40 (2016) 8012-8023.
[18] S. Du, W. Zhang, E. Yue, F. Huang, T. Liang, W.-H. Sun, α,α′-bis(arylimino)-2,3:5,6-bis(pentamethylene)pyridylcobalt chlorides: Synthesis, characterization, and ethylene polymerization behavior, Eur. J. Inorg. Chem. 2016 (2016) 1748-1755.
[19] F. He, W. Zhao, X. Cao, T. Liang, C. Redshaw, W.-H. Sun, 2-[1-(2,6-dibenzhydryl-4-chlorophenylimino)ethyl]-6-[1-aryliminoethyl]pyridyl cobalt dichlorides: Synthesis, characterization and ethylene polymerization behavior, J. Organomet. Chem. 713 (2012) 209-216.
[20] S. Jie, S. Zhang, W.-H. Sun, X. Kuang, T. Liu, J. Guo, Iron(II) complexes ligated by 2-imino-1,10-phenanthrolines: Preparation and catalytic behavior toward ethylene oligomerization, J. Mol. Catal. A: Chem. 269 (2007) 85-96.
[21] J.D.A. Pelletier, Y.D.M. Champouret, J. Cadarso, L. Clowes, M. Gañete, K. Singh, V. Thanarajasingham, G.A. Solan, Electronically variable imino-phenanthrolinyl-cobalt complexes; synthesis, structures and ethylene oligomerisation studies, J. Organomet. Chem. 691 (2006) 4114-4123.
[22] W.-H. Sun, P. Hao, S. Zhang, Q. Shi, W. Zuo, X. Tang, Iron(II) and cobalt(II) 2-(benzimidazolyl)-6-(1-(arylimino)ethyl)pyridyl complexes as catalysts for ethylene oligomerization and polymerization, Organometallics 26 (2007) 2720-2734.
[23] K. Wang, P. Hao, D. Zhang, W.-H. Sun, Tridentate NˆNˆN iron(II) and cobalt(II) complexes of ion-paired structures: Synthesis, characterization and magnetism, J. Mol. Struct. 890 (2008) 95-100.
[24] S. Zhang, W.-H. Sun, T. Xiao, X. Hao, Ferrous and cobaltous chlorides bearing 2,8-

bis(imino)quinolines: Highly active catalysts for ethylene polymerization at high temperature, Organometallics 29 (2010) 1168-1173.
[25] V.K. Appukuttan, Y. Liu, B.C. Son, C.-S. Ha, H. Suh, I. Kim, Iron and cobalt complexes of 2,3,7,8-tetrahydroacridine-4,5(1*H*,6*H*)-diimine sterically modulated by substituted aryl rings for the selective oligomerization to polymerization of ethylene, Organometallics 30 (2011) 2285-2294.
[26] W.-H. Sun, S. Kong, W. Chai, T. Shiono, C. Redshaw, X. Hu, C. Guo, X. Hao, 2-(1-(arylimino)ethyl)-8-arylimino-5,6,7-trihydroquinolylcobalt dichloride: Synthesis and polyethylene wax formation, Appl. Catal., Part A: Gen. 447-448 (2012) 67-73.
[27] Z. Wang, G.A. Solan, Q. Mahmood, Q. Liu, Y. Ma, X. Hao, W.-H. Sun, Bis(imino)pyridines incorporating doubly fused eight-membered rings as conformationally flexible supports for cobalt ethylene polymerization catalysts, Organometallics 37 (2018) 380-389.
[28] Z. Sun, E. Yue, M. Qu, I.V. Oleynik, I.I. Oleynik, K. Li, T. Liang, W. Zhang, W.-H. Sun, 8-(2-cycloalkylphenylimino)-5,6,7-trihydro-quinolylnickel halides: Polymerizing ethylene to highly branched and lower molecular weight polyethylenes, Inorg. Chem. Front. 2 (2015) 223-227.
[29] S.S. Ivanchev, G.A. Tolstikov, V.K. Badaev, I.I. Oleinik, N.I. Ivancheva, D.G. Rogozin, I.V. Oleinik, S.V. Myakin, New bis(arylimino)pyridyl complexes as components of catalysts for ethylene polymerization, Kinetics and Catalysis 45 (2004) 176-182.
[30] H. Suo, I.V. Oleynik, C. Huang, I.I. Oleynik, G.A. Solan, Y. Ma, T. Liang, W.-H. Sun, Ortho-cycloalkyl substituted N,N' -diaryliminoacenaphthene-Ni(II) catalysts for polyethylene elastomers; exploring ring size and temperature effects, Dalton Trans. 46 (2017) 15684-15697.
[31] Z. Sun, F. Huang, M. Qu, E. Yue, I.V. Oleynik, I.I. Oleynik, Y. Zeng, T. Liang, K. Li, W. Zhang, W.-H. Sun, Targeting polyethylene waxes: 9-(2-cycloalkylphenylimino)-5,6,7,8-tetrahydrocycloheptapyridylnickel halides and their use as catalysts for ethylene polymerization, RSC Adv. 5 (2015) 77913-77921.
[32] I.I. Oleinik, I.V. Oleinik, I.B. Abdrakhmanov, S.S. Ivanchev, G.A. Tolstikov, Design of arylimine postmetallocene catalytic systems for olefin polymerization: I. Synthesis of substituted 2-cycloalkyl- and 2,6-dicycloalkylanilines, Russ. J. Gen. Chem. 74 (2004) 1423-1427.
[33] G.M. Sheldrick, SHELXT – Integrated space-group and crystalstructure determination, Acta Cryst. A71 (2015) 3-8.
[34] G.M. Sheldrick, Crystal structure refinement with SHELXL, Acta Cryst. C71 (2015) 3-8.
[35] A.M. Archer, M.W. Bouwkamp, M.P. Cortez, E. Lobkovsky, P.J. Chirik, Arene coordination in bis(imino)pyridine iron complexes: Identification of catalyst deactivation pathways in iron-catalyzed hydrogenation and hydrosilation, Organometallics 25 (2006) 4269-4278.
[36] Y. Chen, R. Chen, C. Qian, X. Dong, J. Sun, Halogen-substituted 2,6-bis(imino)pyridyl iron and cobalt complexes: Highly active catalysts for polymerization and oligomerization of ethylene, Organometallics 22 (2003) 4312-4321.
[37] A.K. Tomov, V.C. Gibson, G.J.P. Britovsek, R.J. Long, M. van Meurs, D.J. Jones, K.P. Tellmann, J.J. Chirinos, Distinguishing chain growth mechanisms in metal-catalyzed olefin

oligomerization and polymerization systems: C_2H_4/C_2D_4 co-oligomerization/polymerization experiments using chromium, iron, and cobalt catalysts, Organometallics 28 (2009) 7033-7040.
[38] D.P. Gates, S.A. Svejda, E. Oñate, C.M. Killian, L.K. Johnson, P.S. White, M. Brookhart, Synthesis of branched polyethylene using (α-diimine)nickel(II) catalysts: Influence of temperature, ethylene pressure, and ligand structure on polymer properties, Macromolecules 33 (2000) 2320-2334.
[39] C. Huang, S. Du, G.A. Solan, Y. Sun, W.-H. Sun, From polyethylene waxes to HDPE using an α,α'-bis(arylimino)-2,3:5,6-bis(pentamethylene)pyridyl-chromium(III) chloride pre-catalyst in ethylene polymerisation, Dalton Trans. 46 (2017) 6948-6957.
[40] D.J. Jones, V.C. Gibson, S.M. Green, P.J. Maddox, A.J.P. White, D.J. Williams, Discovery and optimization of new chromium catalysts for ethylene oligomerization and polymerization aided by high-throughput screening, J. Am. Chem. Soc. 127 (2005) 11037-11046.
[41] N.V. Semikolenova, W.-H. Sun, I.E. Soshnikov, M.A. Matsko, O.V. Kolesova, V.A. Zakharov, K.P. Bryliakov, Origin of "multisite-like" ethylene polymerization behavior of the single-site nonsymmetrical bis(imino)pyridine iron(II) complex in the presence of modified methylaluminoxane, ACS Catal. 7 (2017) 2868-2877.
[42] C.W. Extrand, Contact angles and their hysteresis as a measure of liquid−solid adhesion, Langmuir 20 (2004) 4017-4021.
[43] Q. Liu, H. Zou, Y. Shao, Z. Wang, Stable superhydrophobic surface based on low-density polyethylene/ethylene-propylene-diene terpolymer thermoplastic vulcanizate. J. Appl. Polym. Sci. 135 (2018) 46241-46246.
[44] D.K. Owens, R.C. Wendt, Estimation of the surface free energy of polymers, J. Appl. Polym. Sci. 13 (1969) 1741-1747.
[45] X. Lu, C. Zhang, Y. Han, Low-density polyethylene superhydrophobic surface by control of its crystallization behavior, Macromol. Rapid Commun. 25 (2004) 1606-1610.

Captions of Chart, Scheme, Figures and Tables

Chart 1 Fused ligand frameworks derived from parent bis(imino)pyridine **A**

Scheme 1 Synthesis of **Co1** – **Co6** and a representation of $\mathbf{Co_{Me2Ph}}$

Figure 1 OLEX2 representation of Co1; the thermal ellipsoids are shown at the 30% probability level and all hydrogen atoms have been omitted for clarity.

Figure 2 Molecular weight (M_w) and PDI versus a) run temperature b) Al/Co molar ratio and c) run time using **Co3**/MMAO.

Figure 3 Molecular weight (M_w) and PDI versus a) run temperature b) Al/Co molar ratio and c) run time using **Co3**/MAO.

Figure 4 Comparison of the catalytic activities and molecular weight of the polyethylenes generated using **Co1** – **Co6** and $\mathbf{Co_{Me2Ph}}$ with (i) MMAO (left) and (ii) MAO (right) as co-

catalysts.

Figure 5 ^{13}C NMR spectrum of the polyethylene obtained using **Co3**/MAO at 30 ºC (entry 2, in Table 3); recorded in 1,1,2,2-tetrachloroethane-d_2 at 135 ºC (δC 73.8).

Figure 6 ^{13}C NMR spectra of the polyethylene obtained using a) **Co3**/MMAO b) **Co2**/MMAO and c) **Co6**/MMAO after 30 minutes at 20 ºC (entries 3, 2, and 6, Table 4); all spectra recorded in 1,1,2,2-tetrachloroethane-d_2 at 135 ºC (δC 73.8).

Figure 7 ^{13}C NMR spectrum of the polyethylene obtained with **Co3**/MMAO at 60 ºC (entry 5, in Table 2); recorded in 1,1,2,2-tetrachloroethane-d_2 at 135 ºC (δC 73.8).

Figure 8 The water contact angles for the polyethylenes obtained using a) **Co3**/MMAO at 60 ºC, b) **Co1**/MMAO at 20 ºC and c) **Co2**/MMAO at 20 ºC

Table 1 Ethylene polymerization by **Co3**/MMAO

Table 2 Ethylene polymerization by **Co3**/MAO

Table 3 Ethylene polymerization using **Co1** – **Co6** and **Co$_{Me2Ph}$** using either MMAO or MAO

Supporting Information

Table S1 Crystal data and structure refinement for **Co1**

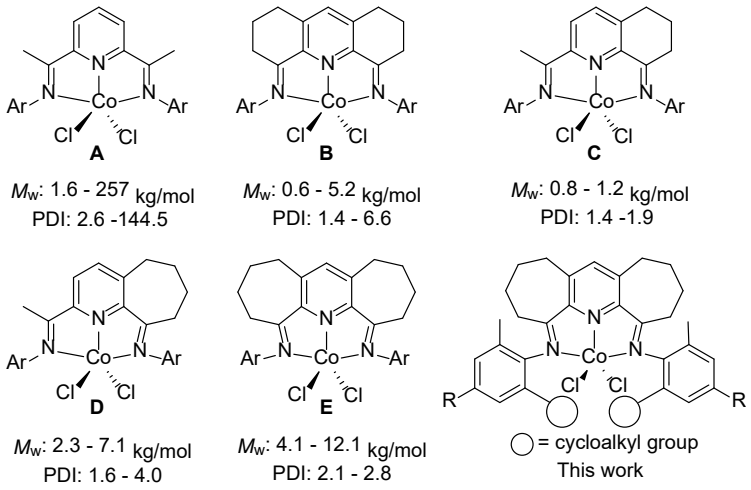

Chart 1 Fused ligand frameworks derived from parent bis(imino)pyridine **A**

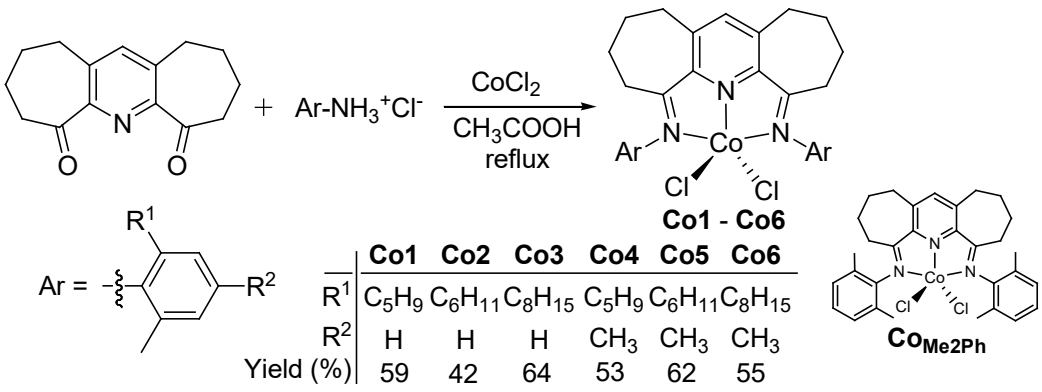

Scheme 1 Synthesis of **Co1** – **Co6** and a representation of **Co**$_{\mathbf{Me2Ph}}$ [18]

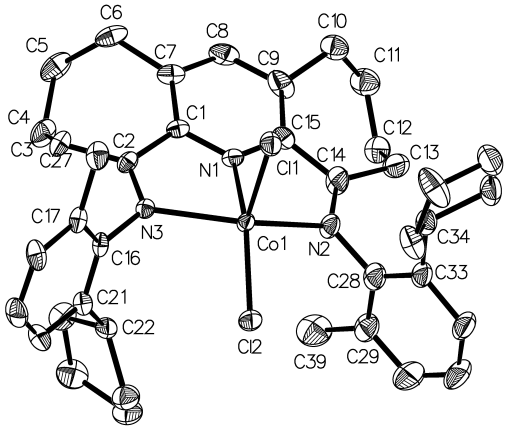

Figure 1 OLEX2 representation of **Co1**; the thermal ellipsoids are shown at the 30% probability level and all hydrogen atoms have been omitted for clarity. Selected bond lengths [Å] and angles [º]: Co1-N1 2.087(4), Co1-N2 2.169(5), Co1-N3 2.174(4), C2-N3 1.282(7), C14-N2 1.291(8), N1-Co1-N2 73.72(18), N1-Co1-N3 74.20(17), N2-Co1-N3 141.51(18), Cl1-Co1-Cl2 115.03(7), C14-C13-C12 110.8(9), C13-C12-C11 113.5(8), C12-C11-C10 116.4(9), C11-C10-C9 109.5(9).

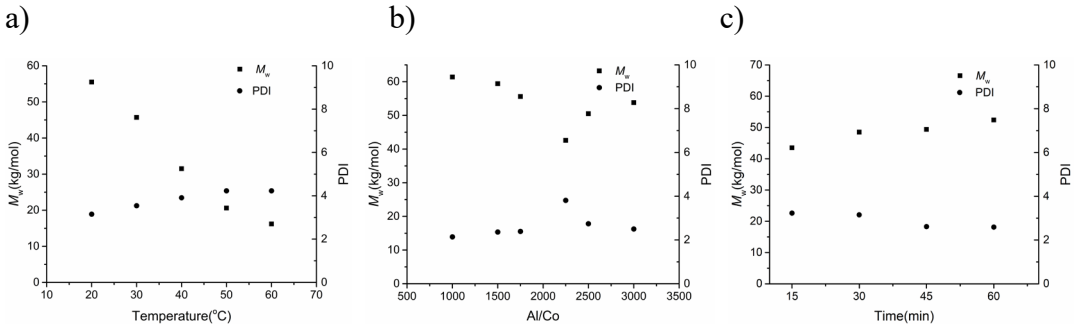

Figure 2 Molecular weight (M_w) and PDI versus a) run temperature b) Al/Co molar ratio and c) run time using **Co3**/MMAO.

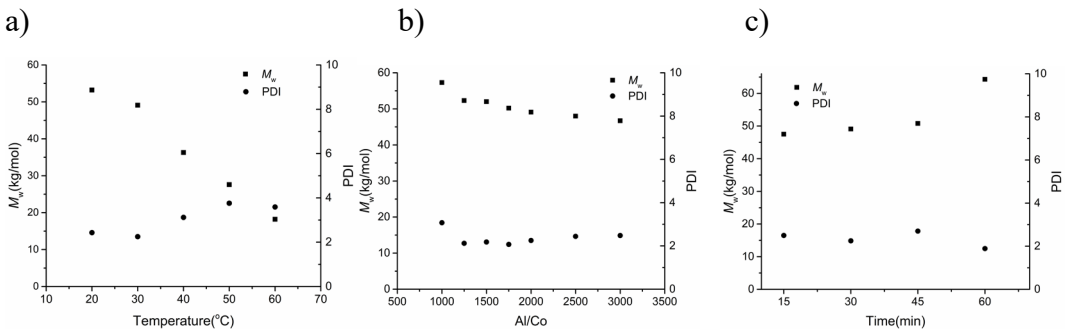

Figure 3 Molecular weight (M_w) and PDI versus a) run temperature b) Al/Co molar ratio and c) run time using **Co3**/MAO.

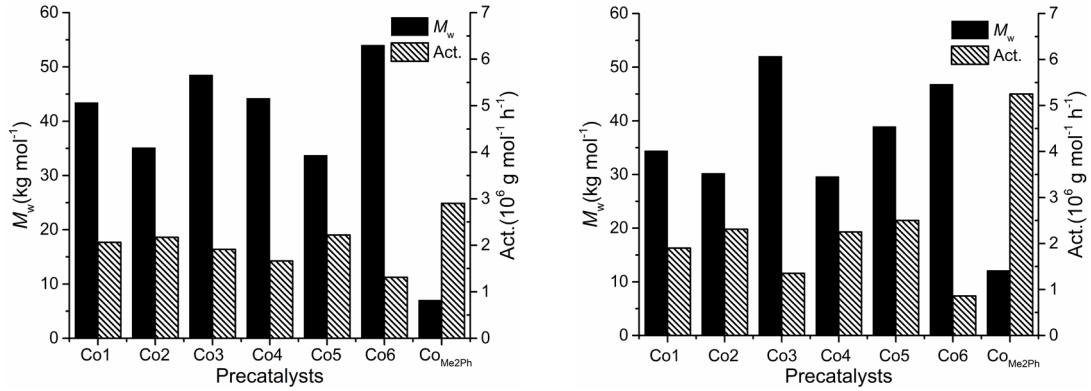

Figure 4 Comparison of the catalytic activities and molecular weight of the polyethylenes generated using **Co1** – **Co6** and **Co_{Me2Ph}** with (i) MMAO (left) and (ii) MAO (right) as co-catalysts.

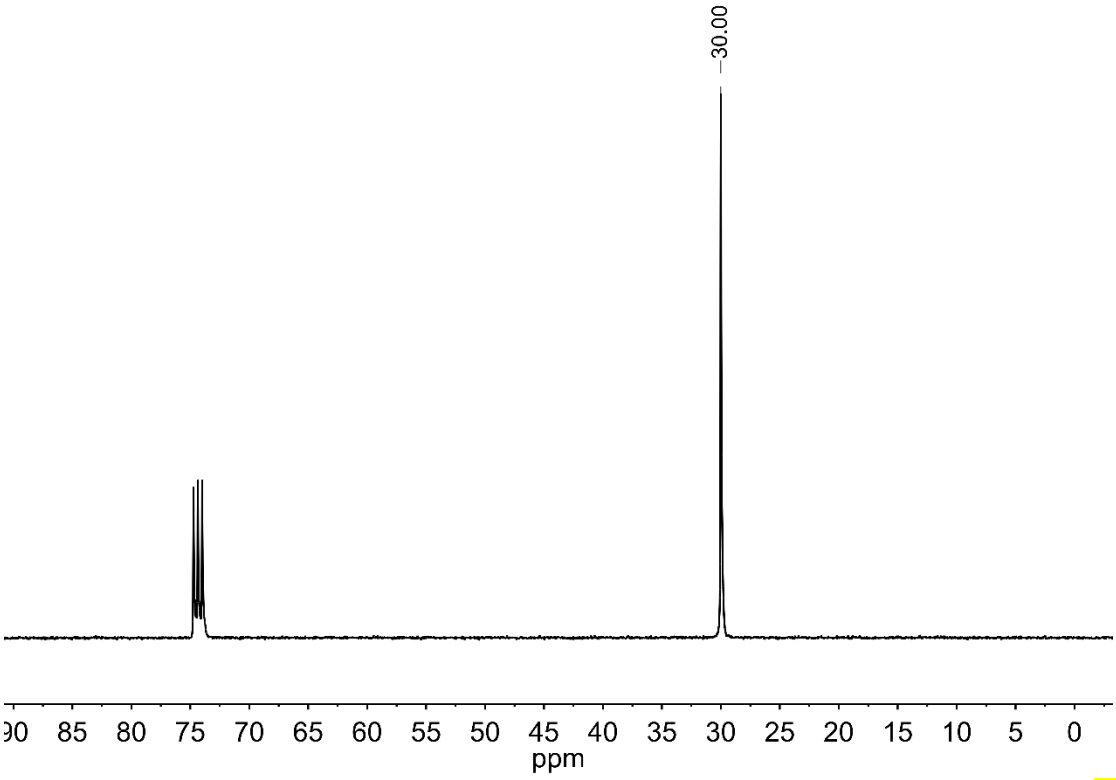

Figure 5 ^{13}C NMR spectrum of the polyethylene obtained using **Co3**/MAO at 30 ºC (entry 2, in Table 2); recorded in 1,1,2,2-tetrachloroethane-d_2 at 135 ºC (δC 73.8).

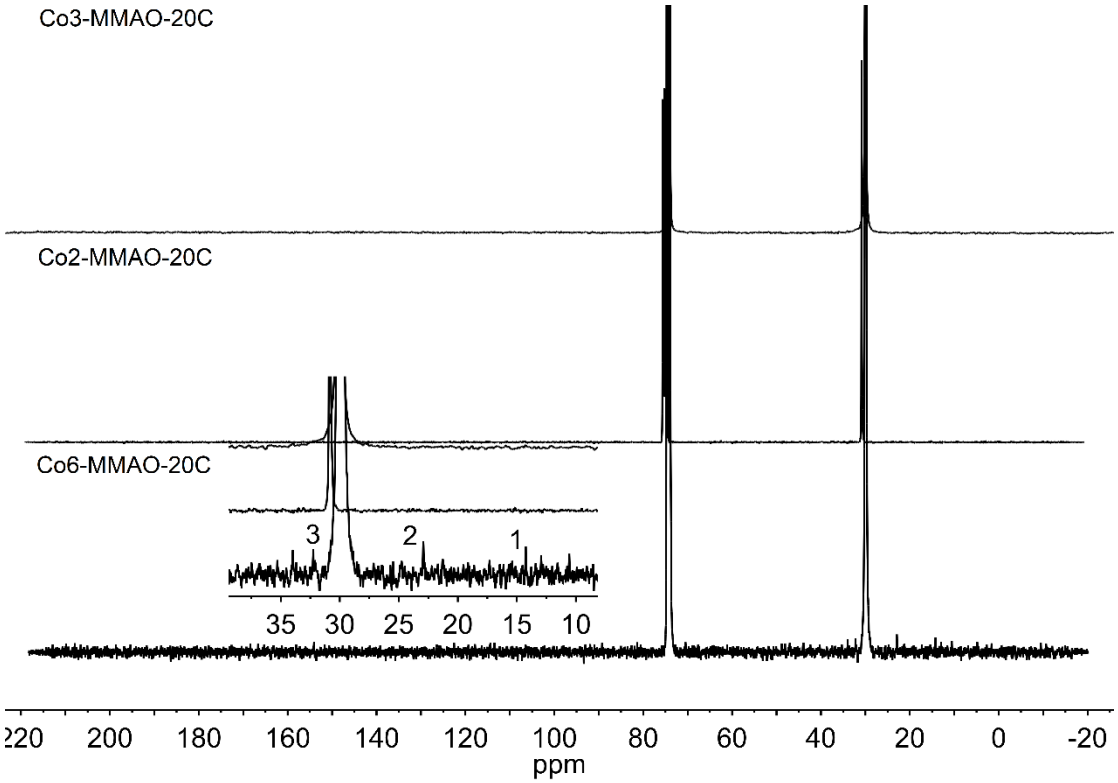

Figure 6 ^{13}C NMR spectra of the polyethylene obtained using a) **Co3**/MMAO b) **Co2**/MMAO and c) **Co6**/MMAO after 30 minutes at 20 ºC (entries 3, 2, and 6, Table 3); all spectra recorded in 1,1,2,2-tetrachloroethane-d_2 at 135 ºC (δC 73.8).

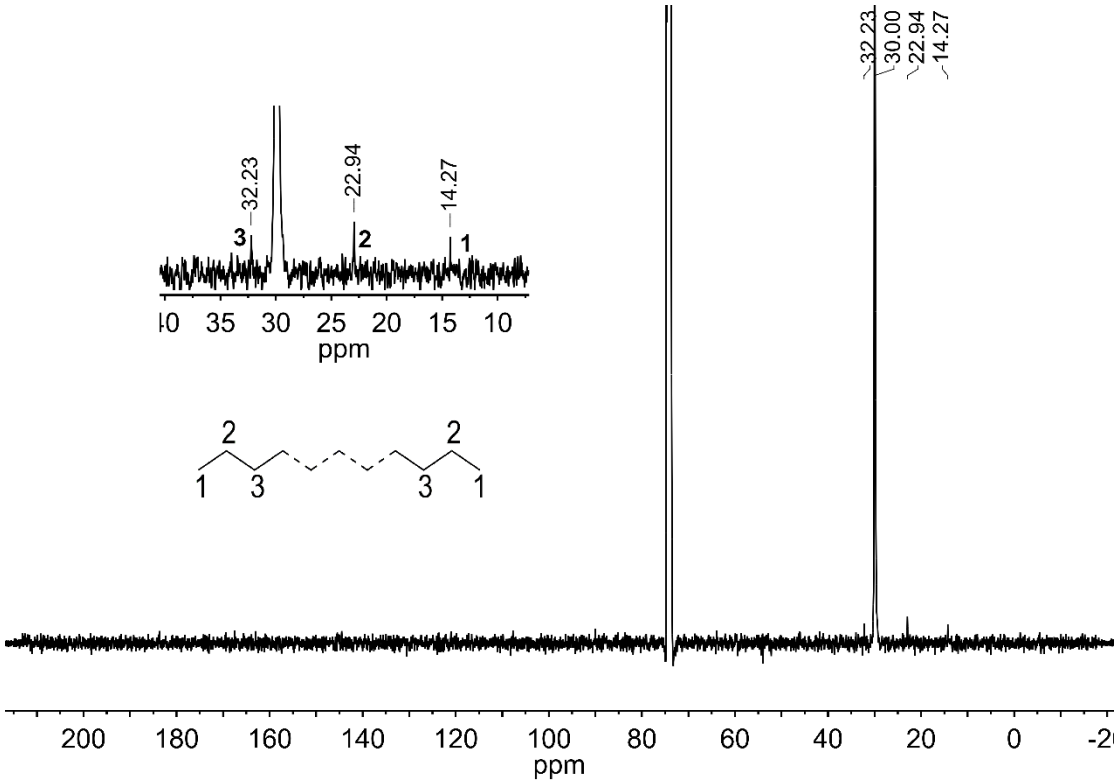

Figure 7 ^{13}C NMR spectrum of the polyethylene obtained with **Co3**/MMAO at 60 ºC (entry 5, in Table 1); recorded in 1,1,2,2-tetrachloroethane-d_2 at 135 ºC (δC 73.8).

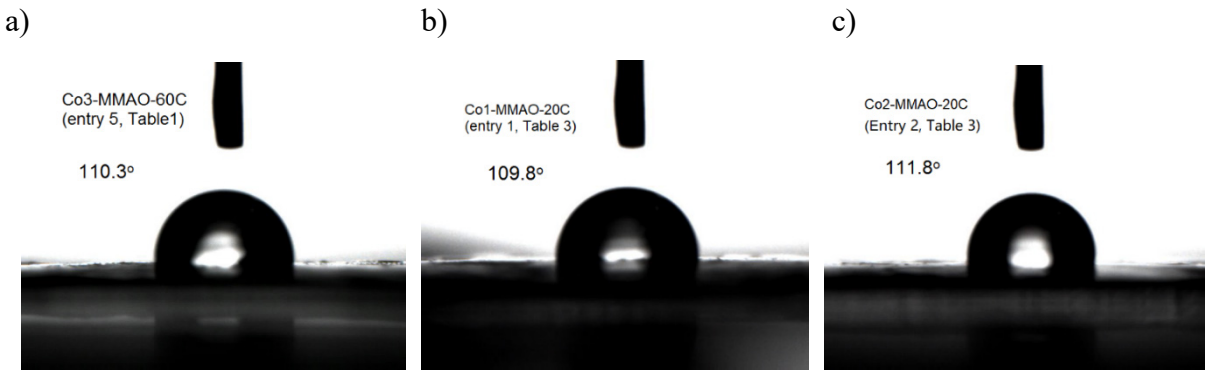

Figure 8 The water contact angles for the polyethylenes obtained using a) **Co3**/MMAO at 60 ºC, b) **Co1**/MMAO at 20 ºC and c) **Co2**/MMAO at 20 ºC

Table 1 Ethylene polymerization by **Co3**/MMAO[a]

Entry	Al/Co	T/°C	t/min	Activity[b]	M_w[c]	M_w/M_n[c]	T_m[d]
1	2000	20	30	1.91	48.5	3.15	134.5
2	2000	30	30	1.39	45.7	3.54	133.9
3	2000	40	30	1.31	31.5	3.91	133.2
4	2000	50	30	0.71	20.6	4.23	132.9
5	2000	60	30	0.27	16.2	4.23	130.7
6	1000	20	30	0.98	61.4	2.14	134.3
7	1500	20	30	1.27	59.4	2.36	133.9
8	1750	20	30	1.56	55.6	2.39	133.8
9	2250	20	30	1.40	42.6	3.81	133.9
10	2500	20	30	1.30	50.5	2.74	134.4
11	3000	20	30	1.16	53.8	2.50	134.8
12	2000	20	15	2.00	43.5	3.23	132.9
13	2000	20	45	1.33	49.4	2.61	134.9
14	2000	20	60	1.05	52.4	2.59	134.7
15[e]	2000	20	30	0.11	52.0	1.93	133.7

[a] Conditions: 3.0 μmol of **Co3**, 10 atm of ethylene, toluene (100 mL) as solvent.

[b] Activity: $\times 10^6$ g PE mol^{-1} (Co) h^{-1}.

[c] M_w in kg mol^{-1}. M_w and M_w/M_n determined by GPC.

[d] Determined by DSC.

[e] 1 atm of ethylene.

Table 2 Ethylene polymerization by **Co3**/MAO[a]

Entry	Al/Co	T/°C	t/min	Activity[b]	M_w[c]	M_w/M_n[c]	T_m[d]
1	2000	20	30	1.13	53.2	2.43	134.7
2	2000	30	30	1.21	49.1	2.25	133.9
3	2000	40	30	0.84	36.3	3.12	133.2
4	2000	50	30	0.79	27.6	3.76	132.4
5	2000	60	30	0.41	18.2	3.59	131.7
6	1000	30	30	0.85	57.3	3.07	135.8
7	1250	30	30	1.12	52.3	2.12	133.6
8	1500	30	30	1.35	52.0	2.18	134.3
9	1750	30	30	1.20	50.2	2.07	133.8
10	2500	30	30	1.18	48.0	2.44	134.3
11	3000	30	30	0.97	46.7	2.48	133.3
12	1500	30	15	1.80	47.5	2.50	134.8
13	1500	30	45	1.14	52.7	2.70	134.5
14	1500	30	60	0.91	64.3	1.89	133.6
15[e]	1500	30	30	0.17	58.7	1.94	133.7

[a] Conditions: 3.0 μmol of **Co3**, 10 atm of ethylene, toluene (100 mL) as solvent.

[b] Activity: $\times 10^6$ g PE mol^{-1} (Co) h^{-1}.

[c] M_w in kg mol^{-1}. M_w and M_w/M_n determined by GPC.

[d] Determined by DSC.

[e] 1 atm of ethylene.

Table 3 Ethylene polymerization using **Co1** – **Co6** and $\mathbf{Co_{Me2Ph}}$ using either MMAO or MAO[a]

Entry	Precat.	Co-cat.	Al/Co	T/°C	Activity[b]	M_w[c]	M_w/M_n [c]	T_m[d]	$\Delta H_f(T_m)$[d]
1	**Co1**	MMAO	2000	20	2.06	43.4	2.08	136.8	176.7
2	**Co2**	MMAO	2000	20	2.17	35.1	2.28	133.2	188.0
3	**Co3**	MMAO	2000	20	1.91	48.5	3.15	134.5	185.3
4	**Co4**	MMAO	2000	20	1.66	44.2	2.13	136.0	204.7
5	**Co5**	MMAO	2000	20	2.22	33.7	2.29	135.6	176.4
6	**Co6**	MMAO	2000	20	1.31	54.0	2.45	134.6	198.0
7	$\mathbf{Co_{Me2Ph}}$	MMAO	2000	20	2.90	6.95	2.32	128.0	197.9
8	**Co1**	MAO	1500	30	1.90	34.4	2.20	133.5	204.6
9	**Co2**	MAO	1500	30	2.31	30.2	2.16	133.4	235.4
10	**Co3**	MAO	1500	30	1.35	52.0	2.18	134.3	188.7
11	**Co4**	MAO	1500	30	2.25	29.6	2.34	134.4	235.7
12	**Co5**	MAO	1500	30	2.50	38.9	1.86	135.3	199.8
13	**Co6**	MAO	1500	30	0.86	46.8	2.10	134.8	221.3
14	$\mathbf{Co_{Me2Ph}}$	MAO	1500	30	5.25	12.1	1.76	130.1	177.2

[a] Conditions: 3.0 μmol of precatalyst, MMAO or MAO as co-catalyst, 30 min run time, 10 atm of ethylene and toluene (100 mL) as solvent.

[b] Activity: $\times 10^6$ g PE mol^{-1} (Co) h^{-1}.

[c] M_w in kg mol^{-1}. M_w and M_w/M_n determined by GPC.

[d] Determined by DSC.